

Abstract

We discuss Greenland ice sheet (GrIS) surface mass balance (SMB) differences between the updated polar version of the regional climate model RACMO2.3 and the previous version RACMO2.1. Among other revisions, the updated model includes an adjusted rainfall-to-snowfall conversion, producing exclusively snowfall under freezing conditions; this especially favours snowfall in summer when upper air temperatures reach the freezing point. Summer snowfall in the ablation zone of the GrIS has a pronounced effect on melt rates, affecting modelled GrIS SMB in two ways. By covering relatively dark ice with highly reflective fresh snow, these summer snowfall have the potential to locally reduce melt rates in the ablation zone of the GrIS through a snow-albedo-melt feedback. At larger scales, SMB changes are driven by differences in orographic precipitation following a shift in large-scale circulation, in combination with enhanced moisture to precipitation conversion for warm to moderately cold conditions. A detailed comparison of model output with long-term observations from automatic weather stations and ablation stakes in west Greenland shows that the model update generally improves the simulated SMB-elevation gradient as well as the representation of the surface energy balance, although significant biases remain.

1 Introduction

Since the mid-1990's, atmospheric and oceanic warming in the Arctic has led to accelerated Greenland ice sheet (GrIS) mass loss (Enderlin and Howat, 2013; Fettweis et al., 2013; Wouters et al., 2013). Combined observational and model studies show that increased meltwater runoff and solid ice discharge through the acceleration of marine-terminating outlet glaciers (Hanna et al., 2009; Nick et al., 2009; Fettweis et al., 2011; Rignot et al., 2011) account for ~ 60 and $\sim 40\%$ of the recent GrIS mass loss, respectively (Rignot et al., 2008; Van den Broeke et al., 2009; Enderlin and Howat, 2013).

Impact of summer snowfall events on GrIS SMB

B. Noël et al.

Title Page

Abstract

Introduction

Conclusions

References

Tables

Figures



Back

Close

Full Screen / Esc

Printer-friendly Version

Interactive Discussion



Since surface melt over the GrIS is mainly driven by the absorption of shortwave radiation (Van den Broeke et al., 2008), surface albedo is a primary factor governing ice sheet surface mass balance (SMB) (Bougamont et al., 2005; Tedesco et al., 2011; Fitzgerald et al., 2012) and surface energy balance (SEB) (Tedesco et al., 2008; Van Angelen et al., 2012). Ice albedo is mainly a function of impurity content, while snow albedo is sensitive to several snow physical properties, e.g. grain size, liquid water content and soot concentration. Satellite and in-situ observations have revealed a general decay of GrIS surface albedo in recent years (Box et al., 2012; Stroeve et al., 2013). In the ablation zone, this decrease is mainly caused by the prolonged exposure of dark, bare ice (Fettweis et al., 2011; Tedesco et al., 2011). In the accumulation zone, enhanced melt-driven snow metamorphism has also led to a surface darkening (Box et al., 2012). Here, the positive melt-albedo feedback is especially pronounced: once snow melts, snow grain size quickly increases, reducing the surface albedo, enhancing the absorption of solar radiation and hence reinforcing surface melting (Stroeve, 2001).

Summer snowfall events have the potential to interrupt this feedback, by covering dark ice and/or metamorphosed snow with a highly reflective fresh snow layer. Greuell and Oerlemans (1986) showed that significant summer snowfall events (> 5 mm w.e.) on an Alpine glacier caused a major reduction in ablation during the following days, subsequently leading to a long-term positive SMB anomaly. They estimated this positive SMB response to be two to three times larger than the mass of deposited solid precipitation. Fettweis et al. (2005) analysed two heavy snowfall events in southeast Greenland at the end of July 1991, using MAR (Modèle Atmosphérique Régional) and AVHRR satellite imagery. These events temporarily raised surface albedo, delaying the appearance of darker bare ice. Based on data from automatic weather stations (AWS), van den Broeke et al. (2011) showed that even minor summer snowfall events (< 5 mm w.e.) can considerably reduce surface melting.

Therefore, an accurate representation of (summer) snowfall events, incoming shortwave radiation and surface processes is essential to model the SMB of the GrIS (Fettweis et al., 2005; Van Angelen et al., 2012). This requires a high-resolution model,

2.2 RACMO2.3 update

The RACMO2 physics package has recently been updated from cycle CY23r4 used in RACMO2.1 (White, 2001) to cycle CY33r1 in the current RACMO2.3 version (ECMWF-IFS, 2008). These updates include major changes in the description of cloud micro-
5 physics, surface and boundary layer turbulence, and radiation transport (Van Wessem et al., 2014). The updated physics package includes an Eddy-Diffusivity Mass Flux scheme (EDMF) (Siebesma et al., 2007), representing turbulence and shallow con-
10 vection in the atmospheric boundary layer. The surface flux computation is based on Monin–Obukhov similarity theory (Beljaars et al., 2004). The new radiation scheme McRad (Morcrette et al., 2008), based on the Monte Carlo Independent Column Ap-
proximation (McICA) (Barker et al., 2008), computes the shortwave and longwave ra-
diation transmission through clouds. In addition, the interaction between shortwave or
15 longwave radiation with multi-layered clouds has been improved by revising the cloud optical properties (ECMWF-IFS, 2008).

The new cloud scheme includes an ice supersaturation parameterisation, which
prolongs the vapour phase at low temperatures (Tompkins et al., 2007). The auto-
conversion coefficient, controlling the conversion rate of water-vapour into precipitation
in convective clouds, has been defined individually for liquid and ice water clouds, fol-
lowing Sundqvist (1978). Moreover, under marginally freezing conditions, precipitation
20 occurs exclusively as snowfall even though the precipitating clouds are mixed phase. In
the previous model version, similar atmospheric conditions could also have resulted in
a mix of liquid and solid precipitation for temperatures above -7°C . The update results
in improved relative contributions of rainfall and snowfall to the total precipitation flux
(Lin et al., 1983). The auto-conversion coefficient now remains constant for liquid water
25 clouds whereas it decreases with temperature for ice clouds. Furthermore, the ice and
liquid water auto-conversion coefficients have been increased in CY33r1 to reduce the
overestimated updraft condensation simulated in previous cycles (ECMWF-IFS, 2008;
Van Wessem et al., 2014). Other minor adjustments have been applied to the physics

TCO

9, 1177–1208, 2015

Impact of summer snowfall events on GrIS SMB

B. Noël et al.

Title Page

Abstract

Introduction

Conclusions

References

Tables

Figures

◀

▶

◀

▶

Back

Close

Full Screen / Esc

Printer-friendly Version

Interactive Discussion



package and the dynamical core but these are not relevant for this study. A complete overview of all updates is provided by ECMWF-IFS (2008) and Van Meijgaard et al. (2012).

2.3 RACMO2 simulations set-up

In RACMO2.3, identical domain and resolutions (~ 11 km, 40 vertical layers) were used as in the previous RACMO2.1 simulation (Van Angelen et al., 2013). The integration domain includes the GrIS, the Canadian Arctic Archipelago, Iceland and Svalbard. At the lateral atmospheric boundaries, RACMO2.3 is forced at 6 hourly time interval by reanalysis data of ERA-40 (Uppala et al., 2005) for the period 1958–1978 and ERA-Interim (Stark et al., 2007; Dee et al., 2011) for the period 1979–2013. Sea surface temperature and sea ice cover are prescribed from the same reanalysis data. Since RAMO2.1 has been forced by ERA-Interim data only for the period 1990–2012 and by ERA-40 prior to that, we compare model results for the overlapping period (1990–2012). This period coincides with long-term SMB and AWS measurements performed along the K-transect in west Greenland, which are therefore used for model evaluation (see Sect. 2.4).

In both RACMO2 versions, Moderate Resolution Imaging Spectroradiometer (MODIS) albedo products (Stroeve et al., 2005) are used to prescribe a background ice albedo, which is assumed to vary in space but to be constant in time. MODIS products were retrieved from satellite observations at 0.05° spatial and 8 day temporal resolutions. The background ice albedo field (Fig. 1) is based on 2001–2010 MODIS values, and ranges from 0.3 to 0.55.

2.4 Observational data

For model evaluation, we use long-term measurements from the K-transect, operated by the Institute for Marine and Atmospheric Research of Utrecht University in the Netherlands (UU/IMAU). The K-transect runs for a distance of approximately 140 km

Impact of summer snowfall events on GrIS SMB

B. Noël et al.

Title Page

Abstract

Introduction

Conclusions

References

Tables

Figures



Back

Close

Full Screen / Esc

Printer-friendly Version

Interactive Discussion



Impact of summer snowfall events on GrlS SMB

B. Noël et al.

Title Page

Abstract

Introduction

Conclusions

References

Tables

Figures

◀

▶

◀

▶

Back

Close

Full Screen / Esc

Printer-friendly Version

Interactive Discussion



from the ice margin through the ablation zone and into the lower accumulation zone of the west Greenland ice sheet along $\sim 67^\circ$ N, covering the elevation interval between 400 and 1850 m a.s.l. (Fig. 1). Since 1990, annual stake measurements have been performed at eight sites along the transect: S4, S5, SHR, S6, S7, S8, S9 and S10 (Van de Wal et al., 2005, 2012). Since August 2003, three AWS with capability to close the SEB have been operated at sites S5 (~ 500 m a.s.l.), S6 (~ 1000 m a.s.l.) and S9 (~ 1500 m a.s.l.) (Van den Broeke et al., 2008, 2009; van den Broeke et al., 2011). Stations S5 and S6 are located in the ablation zone at about 5 and 40 km from the ice sheet margin, while station S9 is located close to the equilibrium line at approximately 90 km from the ice sheet margin. Since 2011, an AWS is also operated in the accumulation zone at S10 (~ 1850 m), about 140 km from the ice sheet margin. At the AWS sites, SEB components are computed using a SEB model that uses as input hourly mean observations of wind, temperature, humidity and radiation components (van den Broeke et al., 2011).

3 Changes in SMB components

3.1 SMB change pattern

Figure 2 shows (a) RACMO2.3 average SMB (1990–2012) and (b) the difference in SMB between RACMO2.3 and RACMO2.1. Both model versions simulate a qualitatively realistic SMB field, with a narrow ablation zone fringing the ice sheet (Fig. 2). The ablation zone is widest (~ 100 – 150 km) in the southwest and northeast, but too narrow in the southeast to be resolved at a resolution of 11 km; in this part of the ice sheet, a steep topography and high precipitation rates induce a large SMB gradients, resulting in an ablation zone of only a few km wide.

The SMB fields from RACMO2.1 and RACMO2.3 are qualitatively similar, but two patterns of change can be discerned (Fig. 2b). First, a large-scale pattern with decreased/increased SMB in the west/east results in enhanced longitudinal SMB gradi-

ents across the main topographical divide. The negative SMB change becomes gradually more pronounced towards the southern and southeastern ice sheet, while the positive anomalies peak in the east. This large-scale pattern can be attributed to changes in the general circulation over the GrIS, as developed in Sect. 3.2.

Secondly, superimposed on this large-scale pattern, Fig. 2b shows pronounced positive SMB changes that are spatially restricted to the ablation and lower accumulation zones of the south-western and north-eastern ice sheet. These regional changes can be ascribed to enhanced summer snowfall in RACMO2.3, following the revised rainfall to snowfall partitioning. These changes are discussed in detail in Sect. 3.3.

3.2 Large-scale precipitation changes

The average mid-tropospheric circulation at 500 hPa is directed southwest-northeast over Greenland (Fig. 3a), resulting in a large-scale precipitation gradient in the same direction. In addition, the proximity of the polar front causes eastwards depressions propagation in south Greenland which advect moist air towards the GrIS, further leading to a pronounced topographically forced precipitation maximum in southeast Greenland.

Compared to RACMO2.1, RACMO2.3 simulates a 0.1 to 0.3 °C cooling in the upper troposphere (above 500 hPa, not shown). The cooling is caused by reduced upper-air condensation, attributed to the introduction of ice supersaturation in the updated physics, leading to increased precipitation in northeast Greenland. Moreover, a lowering of the 500 hPa geopotential height is modelled over the ice sheet with a minimum situated over coastal southeast Greenland (Fig. 3b). The resulting cyclonic circulation anomaly results in stronger onshore flow and increased precipitation in the north-eastern GrIS and a decrease in precipitation in the north-western ice sheet, at the lee side of the main divide. In south Greenland, RACMO2.3 simulates decreased precipitation overall; this is related to enhanced north-westerly advection of colder and drier air masses on the western side of the divide, reinforced offshore katabatic circulation and subsequently weakened onshore flow to the east (Noël et al., 2014).

Impact of summer snowfall events on GrIS SMB

B. Noël et al.

Title Page

Abstract

Introduction

Conclusions

References

Tables

Figures



Back

Close

Full Screen / Esc

Printer-friendly Version

Interactive Discussion



The large-scale circulation anomaly also reduces evaporation over the north Atlantic Ocean, by up to 200 mm w.e. per year (not shown). Moreover, because condensation in the updated scheme is enhanced for moderately cold conditions ($< 10^{\circ}\text{C}$), precipitation over the ocean is enhanced, further limiting precipitation in coastal southeast Greenland. Precipitation differences locally reach 25 %, and integrated over the GrIS the average 1990–2012 precipitation is reduced by 6 %, from 729 Gt yr^{-1} in RACMO2.1 to 687 Gt yr^{-1} in RACMO2.3. Note that the erratic box-like pattern in Fig. 3b results from an error in the meridional momentum advection scheme in RACMO2.1, which is solved in the current formulation.

3.3 Summer snowfall events: the snow-albedo-melt feedback

The enhanced rainfall-to-snowfall conversion in RACMO2.3 favours solid precipitation at the expense of liquid precipitation, especially at higher air temperatures. In winter this has no major impact on the rainfall/snowfall ratio because the air temperature remains mostly below the solid precipitation threshold. In summer (JJA), however, RACMO2.3 predicts locally enhanced snowfall (10–40 mm w.e.), notably in southwest, northeast and northwest Greenland (Fig. 4a). These regional changes are accompanied by an equivalent decrease in rainfall (Fig. 4b), so we conclude that they result from the updated precipitation scheme. The negative (resp. positive) summer snowfall changes in central and southeast (resp. east) Greenland are not compensated by an opposite and equivalent rainfall change; here, precipitation changes are caused by the circulation change discussed in Sect. 3.2.

The regions experiencing increased summer snowfall coincide with positive changes in JJA surface albedo (Fig. 4c). The impact of summer snowfall on albedo is largest in the ablation zone, where the amount of absorbed shortwave radiation is reduced by a factor of ~ 3 when dark bare ice (albedo ~ 0.3 – 0.55) is covered by fresh snow (albedo ~ 0.85). As a consequence, meltwater runoff, which in RACMO2 is assumed to occur instantaneously over bare ice, is also substantially reduced (Fig. 4d). Note that this reduction in runoff (40–160 mm w.e.) in magnitude significantly exceeds the snow-

Impact of summer snowfall events on GrIS SMB

B. Noël et al.

Title Page

Abstract

Introduction

Conclusions

References

Tables

Figures



Back

Close

Full Screen / Esc

Printer-friendly Version

Interactive Discussion



fall anomaly in Fig. 4a (5–30 mm w.e.), stressing the importance of the snow-albedo-melt feedback mechanism, in line with previously published results for valley glaciers (Greuell and Oerlemans, 1986). The pronounced runoff reductions are mirrored in the map of SMB change (Fig. 2b).

4 Evaluation using observational data: a case study for west Greenland

4.1 SEB evaluation along the K-transect

In this section, we compare modelled and observed monthly mean SEB components (2004–2012) along the K-transect, conveniently situated in a region of west Greenland where significant SMB changes occur (Fig. 2b). The SEB is given by:

$$\begin{aligned} M &= SW_d + SW_u + LW_d + LW_u + SHF + LHF + G \\ &= SW_n + LW_n + SHF + LHF + G \end{aligned}$$

where: SW_d and SW_u are the downward and upward shortwave radiations ($W m^{-2}$), LW_d and LW_u are the downward and upward longwave radiations ($W m^{-2}$), SHF and LHF are the sensible and latent turbulent heat fluxes ($W m^{-2}$), G is the ground heat flux ($W m^{-2}$), and SW_n and LW_n are the net short/longwave radiations ($W m^{-2}$).

SEB data from the AWS at S6 are not used because of gaps in the time series at this location. Figure 5 and Tables 1 to 3 show observed and modelled monthly mean SEB components, surface albedo, melt energy and the differences for the period 2004–2012 (S5 and S9) and 2010–2012 (S10). For station S9, a distinction is made between the sub-periods 2004–2008 and 2009–2012; this is deemed relevant because of the significantly warmer summer conditions near the surface and in the upper atmosphere during the latter period. Figure 5a, c, e and g shows that there is qualitative agreement between the modelled and observed seasonal cycle of the SEB in the ablation, equilibrium and accumulation zones. However, important biases remain, as discussed below.

Impact of summer snowfall events on GrlS SMB

B. Noël et al.

Title Page

Abstract

Introduction

Conclusions

References

Tables

Figures

◀

▶

◀

▶

Back

Close

Full Screen / Esc

Printer-friendly Version

Interactive Discussion



Impact of summer snowfall events on GrIS SMB

B. Noël et al.

Title Page

Abstract

Introduction

Conclusions

References

Tables

Figures

◀

▶

◀

▶

Back

Close

Full Screen / Esc

Printer-friendly Version

Interactive Discussion



mer atmospheric temperatures in 2009–2012 were too high for the new precipitation scheme to enhance snowfall. The bias in surface albedo between models and observations is ascribed to a too high prescribed bare ice albedo of about 0.55 (Fig. 1). In fact, both RACMO2 versions fail to reproduce the recent decline in summer ice albedo at S9, which is transforming from an accumulation towards an ablation site. In recent warm summers, the exposed bare ice surface at S9 showed albedo values of about 0.43 and 0.45 in 2010 and 2012 respectively, while RACMO2 is restricted to 0.55 since no ice albedo could be derived from MODIS imagery at this location (Fig. 5f).

4.1.3 Accumulation zone (S10)

At S10, biases in shortwave fluxes are greatly reduced but again the negative LW_d bias persists (Table 3). In winter this is mainly compensated by an overestimated SHF, but not so in summer (Fig. 5g). In June and July, the representation of albedo has improved, but in August albedo is now overestimated. SW_n remains somewhat too large, however, since LW_n is underestimated, the errors in melt energy are less than 10 W m^{-2} (Fig. 5h). The lower accumulation zone responds similarly to station S9 during 2004–2008 but with a reduced surface albedo sensitivity to summer snowfall, because snow metamorphism is slower in this colder area and snow wetting occurs less frequently.

The generally improved representation of surface snow albedo is attributed to enhanced summer snowfall in RACMO2.3 (see Sect. 3.3), thickening the melting snow cover and allowing a partial recovery of the snow layer over bare ice areas in summer. As a result, snowmelt decreases, further delaying snow cover disappearance and maintaining the surface albedo high until summer snowfall events cease (Fig. 6a). The summer surface albedo increase is further reinforced by a drop in cloud cover. This process reduces LW_d , also decreasing snowmelt at station S9 (Fig. 5d).

Impact of summer snowfall events on GrlS SMB

B. Noël et al.

Title Page

Abstract

Introduction

Conclusions

References

Tables

Figures



Back

Close

Full Screen / Esc

Printer-friendly Version

Interactive Discussion



SMB between 500 and 800 m a.s.l. will require a better representation of SHF which, in combination to SW_d and LW_d , is a primary factor governing melt rate in the lower ablation zone. For elevations between 800 m and the equilibrium line at about 1500 m a.s.l., RACMO2.3 simulates higher SMB values compared to RACMO2.1, resulting mainly from reduced runoff following enhanced summer snowfall through the snow-albedo-melt feedback. The absence of rapid SMB fluctuations in the model between 1400 m a.s.l. and the equilibrium line is clearly related to the fixed upper threshold (0.55) of bare ice albedo prescribed in RACMO2 (Van Angelen et al., 2012). In the accumulation zone (above 1500 m), enhanced snowfall and less runoff have significantly improved the agreement with the K-transect stake observations.

An alternative way to assess model performance is to quantify SMB gradients, here determined by simple least square fitting of a linear function. This yields $3.15 \pm 0.22 \text{ mm w.e. yr}^{-1} \text{ m}^{-1}$ for the observations and 2.73 ± 0.09 and $2.91 \pm 0.07 \text{ mm w.e. yr}^{-1} \text{ m}^{-1}$ for RACMO2.1 and RACMO2.3, respectively; in the updated model, the deviation from the observed gradient has thus decreased from 0.42 to $0.24 \text{ mm w.e. yr}^{-1} \text{ m}^{-1}$, a 43% improvement of the SMB gradient representation.

5 Conclusions

An updated physics package has been implemented in the regional climate model RACMO2.3. Among other changes, the rainfall-to-snowfall conversion has been revised and an ice supersaturation parameterization included, to favour solid over liquid precipitation in summer and reduce the overestimated coastal cloud cover and precipitation simulated in previous versions, respectively (Van de Berg et al., 2006). The subsequent increase in modelled summer snowfall has generally improved the representation of surface energy balance (SEB) and surface mass balance (SMB) along the K-transect in west Greenland. For SEB, these improvements are more pronounced in the lower accumulation zone, where summer temperatures are generally below zero. Close to the equilibrium line, SMB is especially sensitive to snowfall-induced fluctua-

**Impact of summer
snowfall events on
GrIS SMB**

B. Noël et al.

Title Page

Abstract

Introduction

Conclusions

References

Tables

Figures

◀

▶

◀

▶

Back

Close

Full Screen / Esc

Printer-friendly Version

Interactive Discussion



tions in surface albedo. The increase in summer snowfall enhances surface reflectivity, improving the modelled surface albedo in summer as well as SMB representation. However, in recent warm years (e.g. 2010 and 2012) rainfall prevailed even in the new formulation, and no improvement was obtained. At station S5 in the lower ablation zone, summer albedo in RACMO2 is mainly determined by the prescribed MODIS ice albedo, due to near-continuous bare ice exposure. The updated physics in RACMO2.3 have considerably improved the modelled SMB gradient along the K-transect when compared to ablation stake measurements, reducing the SMB gradient bias by 43 %.

Two remaining problems require particular attention in future model updates. Current RCMs still struggle to model the correct cloud cover and cloud type (ice/water) over the GrIS (Box et al., 2012). For instance, both RACMO2 and MAR models underestimate summer LW_d and overestimate SW_d due to an underestimated cloud optical thickness (Ettema et al., 2010; Fettweis et al., 2011). In fact, the inclusion of ice supersaturation in RACMO2.3 might aggravate this problem over the ablation zone, because this change delays cloud formation to higher ice sheet elevations, as was also seen in simulations of Antarctic climate (Van Wessem et al., 2014). Another improvement that is simpler to implement is the background ice albedo, that is currently too low at the ice sheet margin. However, at this point, it is also important to realize that point AWS (SEB) and stake (SMB) measurements may not be representative for a wider area, especially for a spatially heterogeneous variable such as surface albedo. Sub-grid albedo variability may therefore be an important future topic of study. To assess the quality of the simulated SMB in the ablation zone elsewhere in Greenland, an evaluation of RACMO2.3 performance against a much larger dataset of ablation measurements, covering all sectors of the Greenland ice sheet, is currently being conducted.

Acknowledgements. B. Noel, W. J. van de Berg, P. Kuipers Munneke, R. S. W. van de Wal, and M. R. van den Broeke acknowledge support from the Polar Programme of the Netherlands Organization for Scientific Research (NWO/ALW).

References

- Barker, H. W., Cole, J. N. S., Morcrette, J.-J., Pincus, R., Räisänen, P., von Salzenf, K., and Vaillancourt, P. A.: The Monte Carlo independent column approximation: an assessment using several global atmospheric models, *Q. J. Roy. Meteor. Soc.*, 134, 1463–1478, doi:10.1002/qj.303, 2008. 1181
- 5 Beljaars, A. C. M., Brown, A. R., and Wood, N.: A new parametrization of turbulent orographic form drag, *Q. J. Roy. Meteorol. Soc.*, 130, 1327–1347, doi:10.1256/qj.03.73, 2004. 1181
- Bougamont, M., Bamber, J. L., and Greuell, W.: A surface mass balance model for the Greenland Ice Sheet, *J. Geophys. Res.*, 110, F04018, doi:10.1029/2005JF000348, 2005. 1179
- 10 Box, J. E., Fettweis, X., Stroeve, J. C., Tedesco, M., Hall, D. K., and Steffen, K.: Greenland ice sheet albedo feedback: thermodynamics and atmospheric drivers, *The Cryosphere*, 6, 821–839, doi:10.5194/tc-6-821-2012, 2012. 1179, 1191
- Dee, D. P., Uppala, S. M., Simmons, A. J., Berrisford, P., Poli, P., Kobayashi, S., Andrae, U., Balmaseda, M. A., Balsamo, G., Bauer, P., Bechtold, P., Beljaars, A. C. M., van de Berg, L., Bidlot, J., Bormann, N., Delsol, C., Dragani, R., Fuentes, M., Geer, A. J., Haimberger, L., Healy, S. B., Hersbach, H., Hólm, E. V., Isaksen, L., Kållberg, P., Köhler, M., Matricardi, M., McNally, A. P., Monge-Sanz, B. M., Morcrette, J.-J., Park, B.-K., Peubey, C., de Rosnay, P., Tavolato, C., Thépaut, J.-N., and Vitart, F.: The ERA-Interim reanalysis: configuration and performance of the data assimilation system, *Q. J. Roy. Meteorol. Soc.*, 137, 553–597, doi:10.1002/qj.828, 2011. 1182
- 20 ECMWF-IFS: Part IV: Physical Processes (CY33R1), Technical Report, Shinfield Park, Reading, England, 2008. 1181, 1182
- Enderlin, E. M. and Howat, I. M.: Submarine melt rate estimates for floating termini of Greenland outlet glaciers (2000–2010), *J. Glaciol.*, 59, 67–75, doi:10.3189/2013JoG12J049, 2013. 1178
- 25 Ettema, J., van den Broeke, M. R., van Meijgaard, E., van de Berg, W. J., Box, J. E., and Steffen, K.: Climate of the Greenland ice sheet using a high-resolution climate model – Part 1: Evaluation, *The Cryosphere*, 4, 511–527, doi:10.5194/tc-4-511-2010, 2010. 1180, 1191
- Fettweis, X., Gallée, H., Lefebvre, F., and van Ypersele, J.-P.: Greenland surface mass balance simulated by a regional climate model and comparison with satellite-derived data in 1990–30 1991, *Clim. Dynam.*, 24, 623–640, doi:10.1007/s00382-005-0010-y, 2005. 1179

Impact of summer snowfall events on GrIS SMB

B. Noël et al.

Title Page

Abstract

Introduction

Conclusions

References

Tables

Figures



Back

Close

Full Screen / Esc

Printer-friendly Version

Interactive Discussion



Impact of summer snowfall events on GrIS SMB

B. Noël et al.

Title Page

Abstract

Introduction

Conclusions

References

Tables

Figures



Back

Close

Full Screen / Esc

Printer-friendly Version

Interactive Discussion



- Fettweis, X., Tedesco, M., van den Broeke, M., and Ettema, J.: Melting trends over the Greenland ice sheet (1958–2009) from spaceborne microwave data and regional climate models, *The Cryosphere*, 5, 359–375, doi:10.5194/tc-5-359-2011, 2011. 1178, 1179, 1191
- Fettweis, X., Hanna, E., Lang, C., Belleflamme, A., Erpicum, M., and Gallée, H.: *Brief communication* “Important role of the mid-tropospheric atmospheric circulation in the recent surface melt increase over the Greenland ice sheet”, *The Cryosphere*, 7, 241–248, doi:10.5194/tc-7-241-2013, 2013. 1178
- Fitzgerald, P. W., Bamber, J. L., Ridley, J. K., and Rougier, J. C.: Exploration of parametric uncertainty in a surface mass balance model applied to the Greenland Ice Sheet, *J. Geophys. Res.*, 117, F01021, doi:10.1029/2011JF002067, 2012. 1179
- Greuell, W. and Oerlemans, J.: Sensitivity studies with a mass balance model including temperature profile calculations inside the glacier, *Z. Gletscherk. Glazialgeol.*, 22, 101–124, 1986. 1179, 1186
- Hanna, E., Cappelen, J., Fettweis, X., Huybrechts, P., Luckman, A., and Ribergaard, M. H.: Hydrologic response of the Greenland ice sheet: the role of oceanographic warming, *Hydrol. Process.*, 23, 7–30, doi:10.1002/hyp.7090, 2009. 1178
- Kuipers Munneke, P., van den Broeke, M. R., Lenaerts, J. T. M., Flanner, M. G., Gardner, A. S., and van de Berg, W. J.: A new albedo parameterization for use in climate models over the Antarctic ice sheet, *J. Geophys. Res.*, 116, D05114, doi:10.1029/2010JD015113, 2011. 1180
- Lenaerts, J. T. M., van den Broeke, M. R., van Angelen, J. H., van Meijgaard, E., and Déry, S. J.: Drifting snow climate of the Greenland ice sheet: a study with a regional climate model, *The Cryosphere*, 6, 891–899, doi:10.5194/tc-6-891-2012, 2012. 1180
- Lin, Y.-L., Farley, R. D., and Orville, H. D.: Bulk parameterization of the snow field in a cloud model, *J. Appl. Meteorol.*, 22, 1065–1092, doi:10.1175/1520-0450(1983)022<1065:BPOTSF>2.0.CO;2, 1983. 1181
- Morcrette, J.-J., Barker, H. W., Cole, J. N. S., Iacono, M. J., and Pincus, R.: Impact of a new radiation package, McRad, in the ECMWF integrated forecast system, *Mon. Weather Rev.*, 136, 4773–4798, doi:10.1175/2008MWR2363.1, 2008. 1181
- Nick, F. M., Vieli, A., Howat, I. M., and Joughin, I.: Large-scale changes in Greenland outlet glacier dynamics triggered at the terminus, *Nat. Geosci.*, 2, 110–114, doi:10.1038/ngeo394, 2009. 1178
- Noël, B., Fettweis, X., van de Berg, W. J., van den Broeke, M. R., and Erpicum, M.: Sensitivity of Greenland Ice Sheet surface mass balance to perturbations in sea surface temperature and

Impact of summer snowfall events on GrIS SMB

B. Noël et al.

Title Page

Abstract

Introduction

Conclusions

References

Tables

Figures



Back

Close

Full Screen / Esc

Printer-friendly Version

Interactive Discussion



sea ice cover: a study with the regional climate model MAR, *The Cryosphere*, 8, 1871–1883, doi:10.5194/tc-8-1871-2014, 2014. 1184

Rignot, E., Box, J. E., Burgess, E., and Hanna, E.: Mass balance of the Greenland ice sheet from 1958 to 2007, *Geophys. Res. Lett.*, 35, L20502, doi:10.1029/2008GL035417, 2008. 1178

Rignot, E., Velicogna, I., van den Broeke, M. R., Monaghan, A., and Lenaerts, J.: Acceleration of the contribution of the Greenland and Antarctic ice, *Geophys. Res. Lett.*, 38, L05503/1–L05503/5, doi:10.1029/2011GL046583, 2011. 1178

Siebesma, A. P., Soares, P. M. M., and Teixeira, J.: A combined eddy-diffusivity mass-flux approach for the convective boundary layer, *J. Atmos. Sci.*, 64, 1230–1248, doi:10.1175/JAS3888.1, 2007. 1181

Smeets, C. and van den Broeke, M.: Temporal and spatial variations of the aerodynamic roughness length in the ablation zone of the Greenland Ice Sheet, *Bound.-Lay. Meteorol.*, 128, 315–338, doi:10.1007/s10546-008-9291-0, 2008. 1187

Stark, J. D., Office, E. M., Donlon, C. J., Martin, M. J., and McCulloch, M. E.: OSTIA: an operational, high resolution, real time, global sea surface temperature analysis system, *OCEANS 2007 – Europe*, conference publications, Aberdeen, 1–4, doi:10.1109/OCEANSE.2007.4302251, 2007. 1182

Stroeve, J. C.: Assessment of Greenland albedo variability from the advanced very high resolution radiometer Polar Pathfinder data set, *J. Geophys. Res.*, 106, 360–374, doi:10.1016/S0034-4257(00)00179-6, 2001. 1179

Stroeve, J., Box, J. E., Gao, F., Liang, S. L., Nolin, A., and Schaaf, C.: Accuracy assessment of the MODIS 16 day albedo product for snow: comparisons with Greenland in situ measurements, *Remote Sens. Environ.*, 94, 46–60, doi:10.1016/j.rse.2004.09.011, 2005. 1182

Stroeve, J., Box, J. E., Wang, Z., Schaaf, C., and Barretta, A.: Re-evaluation of MODIS MCD43 Greenland albedo accuracy and trends, *Remote Sens. Environ.*, 138, 199–214, doi:10.1016/j.rse.2013.07.023, 2013. 1179

Sundqvist, H.: A parameterization scheme for non-convective condensation including prediction of cloud water content, *Q. J. Roy. Meteorol. Soc.*, 104, 677–690, doi:10.1002/qj.49710444110, 1978. 1181

Tedesco, M., Serreze, M., and Fettweis, X.: Diagnosing the extreme surface melt event over southwestern Greenland in 2007, *The Cryosphere*, 2, 159–166, doi:10.5194/tc-2-159-2008, 2008. 1179

Impact of summer snowfall events on GrIS SMB

B. Noël et al.

Title Page

Abstract

Introduction

Conclusions

References

Tables

Figures



Back

Close

Full Screen / Esc

Printer-friendly Version

Interactive Discussion



Tedesco, M., Fettweis, X., van den Broeke, M. R., van de Wal, R. S. W., Smeets, C. J. P. P., van de Berg, W. J., Serreze, M. C., and Box, J. E.: The role of albedo and accumulation in the 2010 melting record in Greenland, *Environ. Res. Lett.*, 6, 014005, doi:10.1088/1748-9326/6/1/014005, 2011. 1179

5 Tompkins, A. M., Gierens, K., and Rädel, G.: Ice supersaturation in the ECMWF integrated forecast system, *Q. J. Roy. Meteorol. Soc.*, 133, 53–63, doi:10.1002/qj.14, 2007. 1181

Undèn, P., Rontu, L., Järvinen, H., Lynch, P., Calvo, J., Cats, G., Cuxart, J., Eerola, K., Fortelius, C., Garcia-Moya, J. A., Jones, C., Lenderlink, G., McDonald, A., Mcgrath, R., Navascues, B., Nielsen, N. W., Degaard, V., Rodriguez, E., Rummukainen, M., Sattler, K.,
10 Sass, B. H., Savijarvi, H., Schreur, B. W., Sigg, R., and The, H.: HIRLAM-5, Scientific Documentation, technical Report, HIRLAM-5 Project, Norrköping, Sweden, 2002. 1180

Uppala, S. M., Kållberg, P. W., Simmons, A. J., Andrae, U., Bechtold, V. D. C., Fiorino, M., Gibson, J. K., Haseler, J., Hernandez, A., Kelly, G. A., Li, X., Onogi, K., Saarinen, S., Sokka, N., Allan, R. P., Andersson, E., Arpe, K., Balmaseda, M. A., Beljaars, A. C. M., Berg, L. V. D.,
15 Bidlot, J., Bormann, N., Caires, S., Chevallier, F., Dethof, A., Dragosavac, M., Fisher, M., Fuentes, M., Hagemann, S., Hólm, E., Hoskins, B. J., Isaksen, L., Janssen, P. A. E. M., Jenne, R., McNally, A. P., Mahfouf, J.-F., Morcrette, J.-J., Rayner, N. A., Saunders, R. W., Simon, P., Ster, A., Trenberth, K. E., Untch, A., Vasiljevic, D., Viterbo, P., and Woollen, J.: The ERA-40 re-analysis, *Q. J. Roy. Meteorol. Soc.*, 131, 2961–3012, 2005. 1182

20 van Angelen, J. H., Lenaerts, J. T. M., Lhermitte, S., Fettweis, X., Kuipers Munneke, P., van den Broeke, M. R., van Meijgaard, E., and Smeets, C. J. P. P.: Sensitivity of Greenland Ice Sheet surface mass balance to surface albedo parameterization: a study with a regional climate model, *The Cryosphere*, 6, 1175–1186, doi:10.5194/tc-6-1175-2012, 2012. 1179, 1180, 1189, 1190

25 Van Angelen, J. H., van den Broeke, M. R., Wouters, B., and Lenaerts, J. T. M.: Contemporary (1969–2012) evolution of the climate and surface mass balance of the Greenland ice sheet, *Surv. Geophys.*, 35, 1155–1174, doi:10.1007/s10712-013-9261-z, 2013. 1182

Van de Berg, W., van den Broeke, M., Reijmer, C., and van Meijgaard, E.: Reassessment of the Antarctic surface mass balance using calibrated output of a regional atmospheric climate model, *J. Geophys. Res.*, 111, D11104, doi:10.1029/2005JD006495, 2006. 1190

30 Van den Broeke, M. R., Smeets, P., Ettema, J., and Munneke, P. K.: Surface radiation balance in the ablation zone of the west Greenland ice sheet, *J. Geophys. Res.-Atmos.*, 113, D13105, doi:10.1029/2007JD009283, 2008. 1179, 1183

**Impact of summer
snowfall events on
GrIS SMB**

B. Noël et al.

Title Page

Abstract

Introduction

Conclusions

References

Tables

Figures



Back

Close

Full Screen / Esc

Printer-friendly Version

Interactive Discussion



- Van den Broeke, M. R., Smeets, P., and Ettema, J.: Surface layer climate and turbulent exchange in the ablation zone of the west Greenland ice sheet, *Int. J. Climatol.*, 29, 2309–2323, doi:10.1002/joc.1815, 2009. 1178, 1183
- van den Broeke, M. R., Smeets, C. J. P. P., and van de Wal, R. S. W.: The seasonal cycle and interannual variability of surface energy balance and melt in the ablation zone of the west Greenland ice sheet, *The Cryosphere*, 5, 377–390, doi:10.5194/tc-5-377-2011, 2011. 1179, 1183
- Van de Wal, R., Greuell, W., van den Broeke, M. R., Reijmer, C. H., and Oerlemans, J.: Surface mass-balance observations and automatic weather station data along a transect near Kangerlussuaq, West Greenland, *Ann. Glaciol.*, 42, 311–316, doi:10.3189/172756405781812529, 2005. 1183
- van de Wal, R. S. W., Boot, W., Smeets, C. J. P. P., Snellen, H., van den Broeke, M. R., and Oerlemans, J.: Twenty-one years of mass balance observations along the K-transect, West Greenland, *Earth Syst. Sci. Data*, 4, 31–35, doi:10.5194/essd-4-31-2012, 2012. 1183
- Van Meijgaard, E., van Uft, L. H., van de Berg, W. J., Bosveld, F. C., van den Hurk, B., Lenderink, G., and Siebesma, A. P.: Technical Report 302: The KNMI Regional Atmospheric Climate Model RACMO version 2.1, Royal Netherlands Meteorological Institute, De Bilt, 2008. 1180
- Van Meijgaard, E., van Uft, L., Lenderink, G., de Roode, S., Wipfler, L., Boers, R., and Timmermans, R. M. A.: Refinement and Application of a Regional Atmospheric Model For Climate Scenario Calculations of Western Europe, *Climate Change Spatial Planning Publication*, KvR 054/12, Wageningen, the Netherlands, 2012. 1182
- van Wessem, J. M., Reijmer, C. H., M. Lenaerts, J. T., van de Berg, W. J., van den Broeke, M. R., and van Meijgaard, E.: Updated cloud physics in a regional atmospheric climate model improves the modelled surface energy balance of Antarctica, *The Cryosphere*, 8, 125–135, doi:10.5194/tc-8-125-2014, 2014. 1181, 1191
- White, P. W.: Part IV: Physical Processes (CY23R4), Technical Report, Shinfield Park, Reading, England, 2001. 1181
- Wouters, B., Bamber, J. L., van den Broeke, M. R., Lenaerts, J. T. M., and Sasgen, I.: Limits in detecting acceleration of ice sheet mass loss due to climate variability, *Nat. Geosci.*, 6, 613–616, doi:10.1038/ngeo1874, 2013. 1178

Impact of summer
snowfall events on
GrIS SMB

B. Noël et al.

Table 1. Modelled and observed monthly mean SEB components and statistics of the differences (2004–2012) at station S5 (67°06′ N, 50°05′ W, 490 m.a.s.l.) in the ablation zone. Statistics include means of measurements collected at S5, model bias (RACMO2 – observations), SD of the bias, Root Mean Square Difference (RMSD) of the bias as well as determination coefficient between RACMO2.3 (resp. RACMO2.1) and S5 observations.

AWS	S5	OBS.	RACMO2.1				RACMO2.3			
			Variable	unit	mean	bias	σ_{bias}	RMSD	r^2	bias
SW _d	Wm ⁻²	108.7	16.3	18.7	24.8	0.98	26.2	20.8	33.4	0.99
SW _u	Wm ⁻²	69.8	8.5	16.2	18.3	0.95	15.4	18.4	24.0	0.93
LW _d	Wm ⁻²	244.8	-17.2	8.6	19.2	0.97	-18.4	6.9	19.7	0.97
LW _u	Wm ⁻²	280.6	-15.4	9.6	18.1	0.98	-13.9	8.3	16.2	0.98
SHF	Wm ⁻²	37.4	-11.8	19.7	23.0	0.21	-8.9	17.3	19.4	0.46
LHF	Wm ⁻²	-4.1	2.6	5.3	5.9	0.60	1.6	5.0	5.3	0.66
MELT	Wm ⁻²	42.8	-7.8	17.7	19.4	0.96	-5.4	14.2	15.2	0.97
ALB	(-)	0.73	0.03	0.09	0.09	0.73	0.03	0.08	0.09	0.74
T _{2m}	°C	-6.0	-2.7	1.7	3.2	0.99	-2.3	1.1	2.6	0.99

Title Page

Abstract

Introduction

Conclusions

References

Tables

Figures



Back

Close

Full Screen / Esc

Printer-friendly Version

Interactive Discussion



Impact of summer snowfall events on GrIS SMB

B. Noël et al.

Table 3. Same as Table 1 but for station S10 (67°00′ N, 47°01′ W, 1850 m a.s.l.) in the accumulation zone. SEB components include monthly mean data for the period 2004–2012.

Variable	AWS	S10	OBS.	RACMO2.1				RACMO2.3			
				unit	mean	bias	σ_{bias}	RMSD	r^2	bias	σ_{bias}
SW _d		Wm ⁻²	141.5	-11.8	12.9	17.5	0.994	1.8	7.7	7.9	0.997
SW _u		Wm ⁻²	113.8	-15.3	18.0	23.7	0.98	-2.3	12.1	12.4	0.99
LW _d		Wm ⁻²	220.4	-14.1	12.3	18.7	0.92	-14.1	8.9	16.7	0.93
LW _u		Wm ⁻²	252.5	-0.6	5.2	5.2	0.98	-1.6	4.2	4.5	0.99
SHF		Wm ⁻²	11.9	11.6	7.7	13.9	0.64	7.9	5.7	9.8	0.74
LHF		Wm ⁻²	-2.7	-1.5	3.8	4.1	0.41	-2.5	4.0	4.7	0.39
MELT		Wm ⁻²	8.9	2.1	5.9	6.2	0.94	0.7	4.3	4.3	0.94
ALB		(-)	0.86	-0.01	0.04	0.04	0.69	-0.001	0.04	0.04	0.71
T _{2m}		°C	-14.6	1.0	1.4	1.7	0.98	0.5	1.0	1.1	0.99

Title Page

Abstract

Introduction

Conclusions

References

Tables

Figures

◀

▶

◀

▶

Back

Close

Full Screen / Esc

Printer-friendly Version

Interactive Discussion



Impact of summer snowfall events on GrIS SMB

B. Noël et al.

Table 4. Modelled and observed annual mean cumulated SMB and statistics of the differences at S5 (67°06' N, 50°05' W, 490 ma.s.l.), SHR (67°06' N, 49°56' W, 710 ma.s.l.), S6 (67°05' N, 49°24' W, 1010 ma.s.l.), S7 (66°59' N, 49°09' W, 1110 ma.s.l.), S8 (67°00' N, 48°53' W, 1260 ma.s.l.) and S9 (67°03' N, 48°15' W, 1520 ma.s.l.) over 1990–2012; S10 (67°00' N, 47°01' W, 1850 ma.s.l.) covers the period 1994–2010.

Stakes	S5–S10	OBS.	RACMO2.1				RACMO2.3			
			mean	bias	σ_{bias}	RMSD	r^2	bias	σ_{bias}	RMSD
SMB	unit									
S5	m w.e.yr ⁻¹	-3.7	1.0	0.5	1.1	0.36	0.7	0.4	0.8	0.49
SHR	m w.e.yr ⁻¹	-3.1	0.4	0.5	0.6	0.41	0.3	0.4	0.5	0.53
S6	m w.e.yr ⁻¹	-1.7	-0.8	0.6	1.0	0.25	-0.7	0.6	0.9	0.28
S7	m w.e.yr ⁻¹	-1.5	-0.7	0.4	0.9	0.59	-0.6	0.4	0.7	0.66
S8	m w.e.yr ⁻¹	-0.8	-0.7	0.4	0.8	0.55	-0.4	0.4	0.5	0.64
S9	m w.e.yr ⁻¹	-0.1	-0.4	0.2	0.5	0.73	-0.2	0.2	0.3	0.80
S10	m w.e.yr ⁻¹	0.3	-0.03	0.2	0.2	0.34	0.2	0.1	0.3	0.25

Title Page

Abstract

Introduction

Conclusions

References

Tables

Figures

◀

▶

◀

▶

Back

Close

Full Screen / Esc

Printer-friendly Version

Interactive Discussion



Impact of summer snowfall events on GrIS SMB

B. Noël et al.

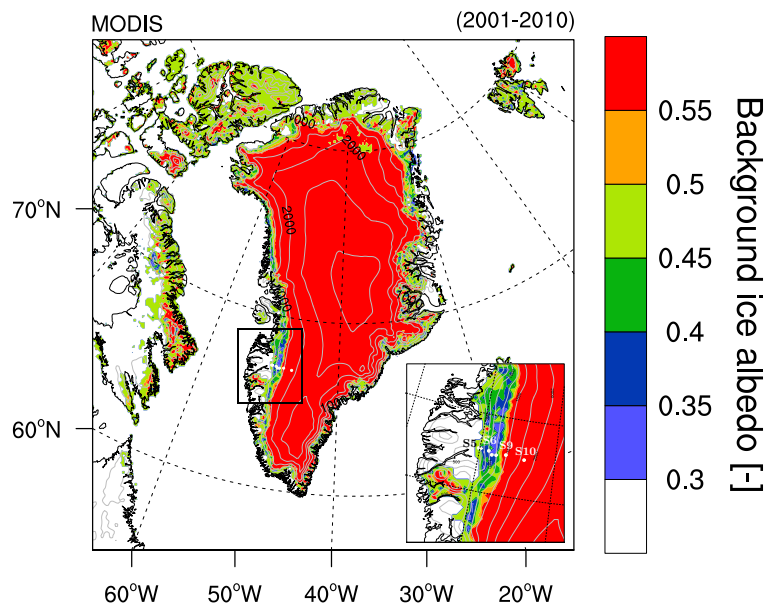


Figure 1. MODIS background ice albedo prescribed in RACMO2.3. The RACMO2 integration domain is displayed as well as the location of the K-transect (white dots, see also inset).

Title Page

Abstract

Introduction

Conclusions

References

Tables

Figures



Back

Close

Full Screen / Esc

Printer-friendly Version

Interactive Discussion



Impact of summer snowfall events on GrIS SMB

B. Noël et al.

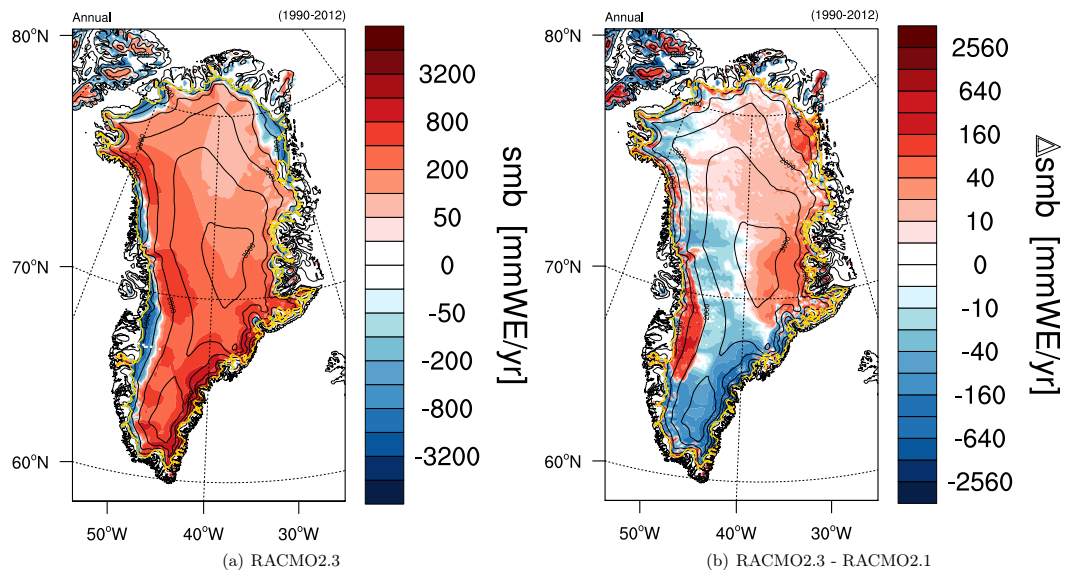


Figure 2. (a) Annual mean cumulated SMB (mm w.e. yr^{-1}) in RACMO2.3; (b) change in annual mean cumulated SMB (mm w.e. yr^{-1}) between RACMO2.3 and RACMO2.1 (1990–2012). The ice sheet margin is displayed in yellow.

Title Page

Abstract

Introduction

Conclusions

References

Tables

Figures



Back

Close

Full Screen / Esc

Printer-friendly Version

Interactive Discussion



Impact of summer snowfall events on GrIS SMB

B. Noël et al.

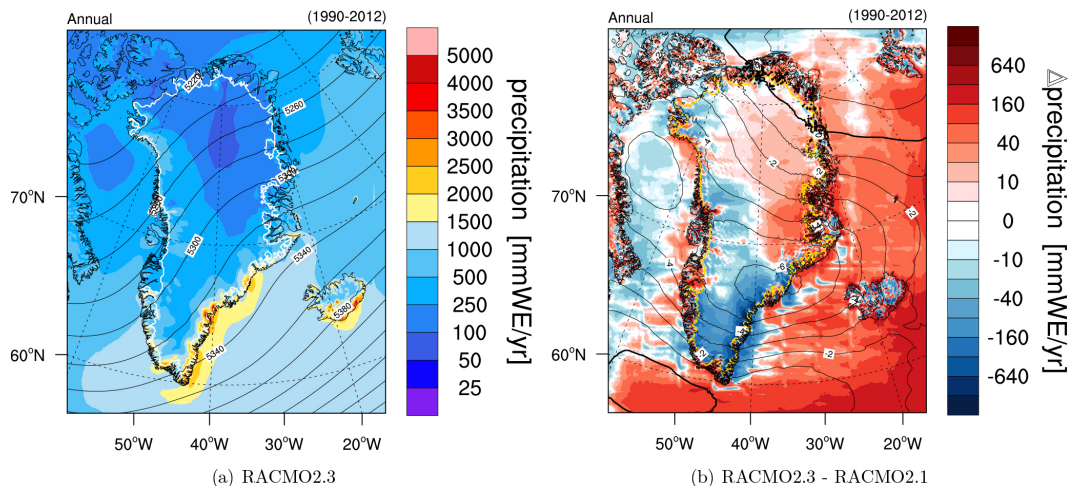


Figure 3. (a) Annual mean cumulated total (rain and snow) precipitation (mm w.e. yr^{-1}) and 500 hPa geopotential height (m) in RACMO2.3; (b) change in annual mean cumulated total precipitation (mm w.e. yr^{-1}) and 500 hPa geopotential height (m) between RACMO2.3 and RACMO2.1 (1990–2012).

Discussion Paper | Discussion Paper | Discussion Paper | Discussion Paper | Discussion Paper

Title Page

Abstract

Introduction

Conclusions

References

Tables

Figures



Back

Close

Full Screen / Esc

Printer-friendly Version

Interactive Discussion



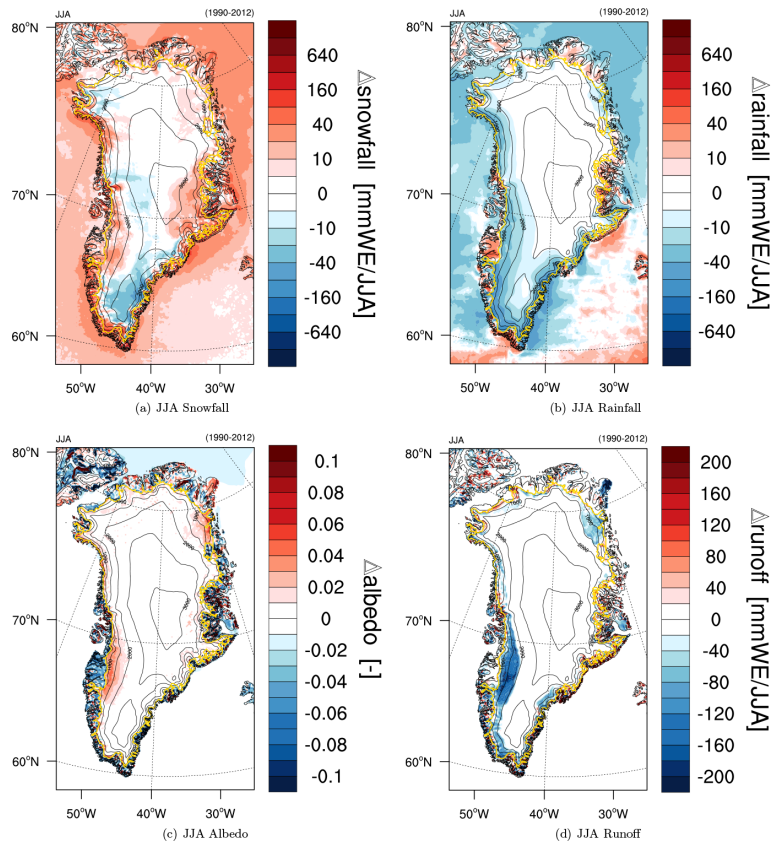


Figure 4. Change in JJA mean (a) cumulated snowfall (mm w.e. JJA^{-1}), (b) rainfall (mm w.e. JJA^{-1}), (c) surface albedo and (d) runoff (mm w.e. JJA^{-1}) between RACMO2.3 and RACMO2.1 (1990–2012).

Impact of summer snowfall events on GrIS SMB

B. Noël et al.

Title Page

Abstract Introduction

Conclusions References

Tables Figures

◀ ▶

◀ ▶

Back Close

Full Screen / Esc

Printer-friendly Version

Interactive Discussion



Impact of summer snowfall events on GrIS SMB

B. Noël et al.

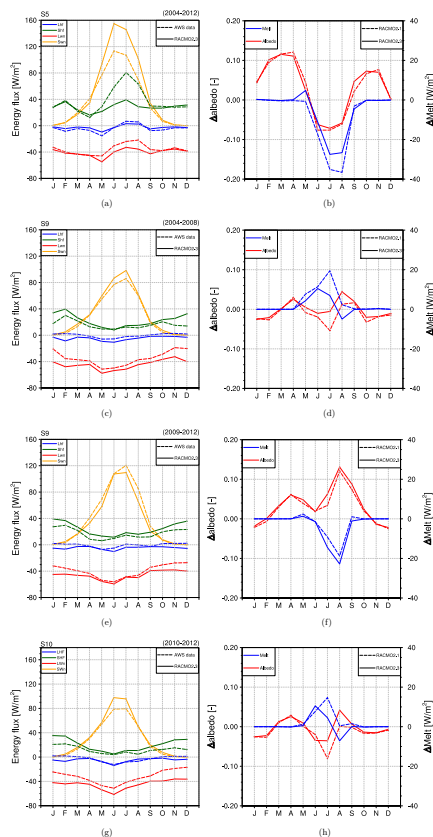


Figure 5. Absolute values of observed and modelled turbulent and net shortwave/longwave fluxes (W m^{-2}) at station **(a)** S5 for 2004–2012, **(c)** S9 for 2004–2008, **(e)** S9 for 2009–2012 and **(g)** S10 for 2010–2012; difference in modelled and observed surface albedo and surface melt energy (W m^{-2}) at stations **(b)** S5, **(d)** S9, **(f)** S9 and **(h)** S10 for the same periods, respectively.

Title Page

Abstract

Introduction

Conclusions

References

Tables

Figures



Back

Close

Full Screen / Esc

Printer-friendly Version

Interactive Discussion



Impact of summer snowfall events on GrIS SMB

B. Noël et al.

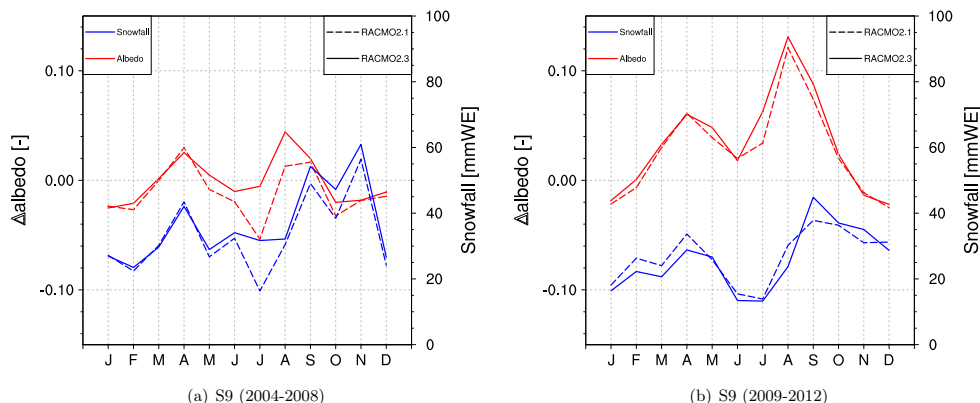


Figure 6. Differences in monthly mean surface albedo between models and S9 measurements combined with absolute monthly mean modelled snowfall for the periods **(a)** 2004–2008 and **(b)** 2009–2012.

Title Page

Abstract

Introduction

Conclusions

References

Tables

Figures

◀

▶

◀

▶

Back

Close

Full Screen / Esc

Printer-friendly Version

Interactive Discussion



Impact of summer snowfall events on GrIS SMB

B. Noël et al.

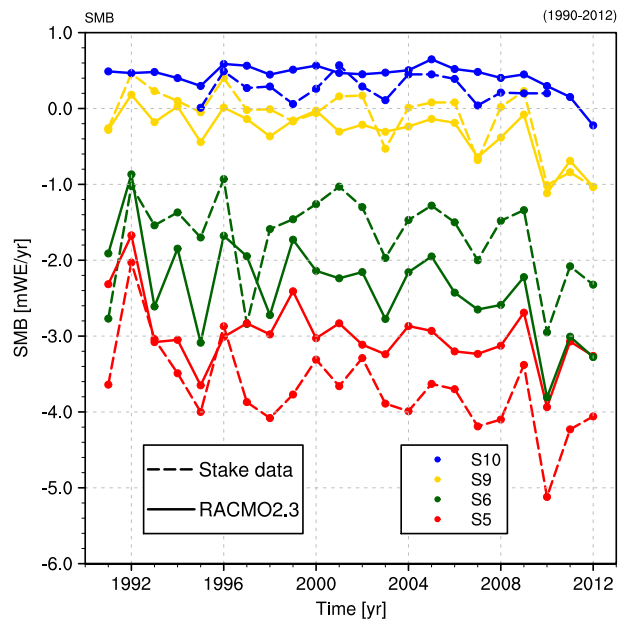


Figure 7. Time series of observed (AWS) and modelled (RACMO2.3 and 2.1) annual mean SMB along the K-transect (m.w.e.yr^{-1}) for the period 1990–2012.

[Title Page](#)[Abstract](#)[Introduction](#)[Conclusions](#)[References](#)[Tables](#)[Figures](#)[◀](#)[▶](#)[◀](#)[▶](#)[Back](#)[Close](#)[Full Screen / Esc](#)[Printer-friendly Version](#)[Interactive Discussion](#)

Impact of summer snowfall events on GrIS SMB

B. Noël et al.

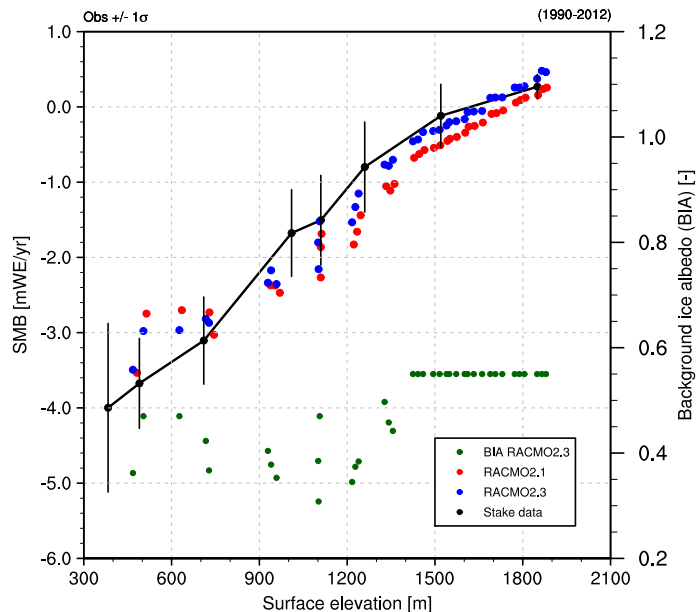


Figure 8. Observed and simulated SMB (m.w.e. yr^{-1}) along the K-transect in western Greenland ($\sim 67^\circ \text{N}$), averaged for the period 1990–2012. The observed SMB (black dots) at S4, S5, SHR, S6, S7, S8, S9 and S10 are based on annual stake measurements. S10 observations cover 1994–2010. The black bars represent the SD ($\pm 1\sigma$) around the 1990–2012 mean value. Modelled SMB at stake sites and intermediate locations are displayed for RACMO2.3 (blue dots) and RACMO2.1 (red dots). MODIS background ice albedo as prescribed in RACMO2.3, is depicted in green (axis on right).

Title Page

Abstract

Introduction

Conclusions

References

Tables

Figures



Back

Close

Full Screen / Esc

Printer-friendly Version

Interactive Discussion

